

Gideon J.J. Steyn and Andreas Roodt, *S. Afr. J. Chem.*, 2001, **54**, 242-263,
 <<http://journals.sabinet.co.za/sajchem/>>,
 <http://ejour.sabinet.co.za/images/ejour/chem/chem_v54_a9.pdf>.
 [formerly: Gideon J.J. Steyn and Andreas Roodt, *S. Afr. J. Chem.*, 2001, **54**, 9. (22 pp.),
 <http://ejour.sabinet.co.za/images/ejour/chem/chem_v54_a9.pdf>.]

RESEARCH ARTICLE

Crystal Structure of $[\text{Rh}(\text{cacsm}-\kappa\text{N},\kappa\text{S})(\text{CO})(\text{PPh}_3)].\text{CH}_3\text{COCH}_3$, (cacsm=methyl 2-(cyclohexylamino)-1-cyclopentene-1-dithiocarboxylate) and Kinetics of Iodomethane Oxidative Addition.

Gideon J.J. Steyn and Andreas Roodt*

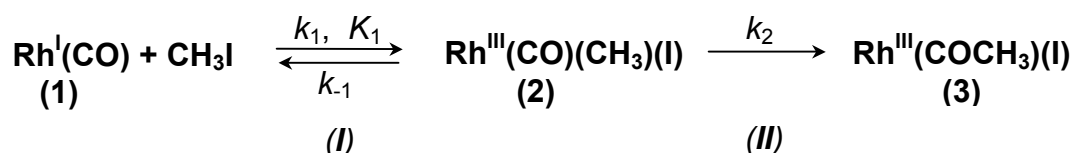
Department of Chemistry, University of the Free State, Bloemfontein 9300, South Africa.

*To whom correspondence should be addressed. Email: roodta@sci.uovs.ac.za

Received 7 November 2000; revised 23 February 2001; accepted 15 April 2001

Abstract

The preparation of the acetone solvate of the title complex (methyl 2-(cyclohexylamino)-1-cyclopentene-1-dithiocarboxylato)- $\kappa\text{N},\kappa\text{S}$ carbonyltriphenyl-phosphinerhodium(I), is described. The X-ray structure of the complex, $[\text{Rh}(\text{cacsm})(\text{CO})(\text{PPh}_3)].\text{CH}_3\text{COCH}_3$ was determined and a final R-value of 4.52% resulted from refinement of 5059 observed reflections. The $[\text{Rh}(\text{cacsm})(\text{CO})(\text{PX}_3)]$ complexes (1), with X = phenyl (Ph), para-chlorophenyl (p-Cl-Ph), para-methoxyphenyl (p-MeO-Ph) and cyclohexyl (Cy), undergo oxidative addition by iodomethane, forming the Rh(III)-alkyl species (2) via an equilibrium step, followed by the formation of the Rh(III)-acyl species (3) according to the reaction:

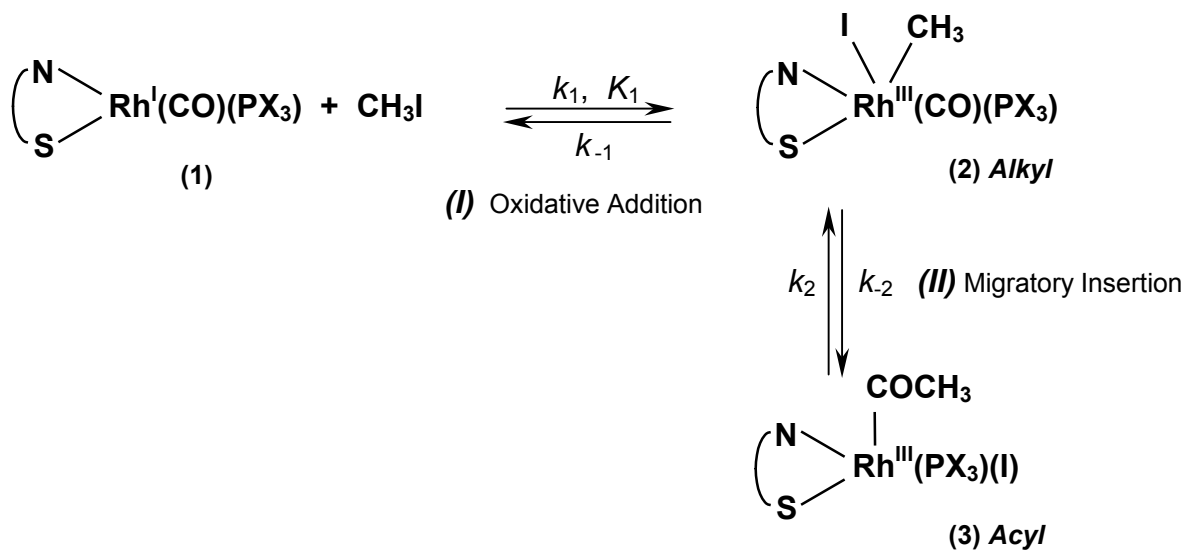


The rate for the oxidative addition reaction increases by one order of magnitude for $P(p\text{-MeO-Ph})_3$ compared with $P(p\text{-Cl-Ph})_3$, while the formation rate of the Rh(III)-acyl species was found to be relatively independent of the higher nucleophilic character of the metal center caused by the increased σ -donating ability of $P(p\text{-MeO-Ph})_3$. Rate and equilibrium constants at 25 °C in chloroform, and activation parameters for $X = (p\text{-MeO-Ph})$ are as follows: $k_1 = (1.17 \pm 0.04) \times 10^{-1} \text{ L mol}^{-1} \text{ s}^{-1}$; $k_{-1} = (1.2 \pm 0.3) \times 10^{-2} \text{ s}^{-1}$; $k_2 = (2.9 \pm 0.1) \times 10^{-3} \text{ s}^{-1}$, $K_1 = (12 \pm 2) \text{ L mol}^{-1}$, $\Delta H^\ddagger(k_1) = (38 \pm 7) \text{ kJ mol}^{-1}$, $\Delta S^\ddagger(k_1) = (-172 \pm 26) \text{ J K}^{-1} \text{ mol}^{-1}$. A one order of magnitude decrease in the oxidative addition equilibrium constant, K_1 , was observed in ethyl acetate as solvent compared with acetone and chloroform.

Keywords Oxidative addition; Rhodium; crystal structure; kinetics.

1. Introduction

The application of rhodium in catalysis is widespread, ranging amongst others from the production of acetic acid¹ to hydrogenation,² and new catalysts, as well as catalyst precursors, are constantly required. The $[\text{Rh}(\text{BID})(\text{CO})(\text{PPh}_3)]$ complexes (BID = monocharged bidentate ligand) can be activated towards iodomethane oxidative addition by the introduction of the methyl ester of 2-(methylamino)-1-cyclopentene-1-dithiocarboxylic acid (macsm) as N,S chelate.^{3,4} Further variation of electron density was accomplished on the metal center by introduction of different substituents on the aminocyclopentene-dithiocarboxylato backbone and resulted in an even greater enhancement of the oxidative addition rate in the case when 2-(cyclohexylamino)-1-cyclopentene 1-dithiol (macshH)⁵ was used as the N,S-bidentate ligand. This study confirmed the general two-step mechanism presented in Scheme 1, in which an equilibrium between the Rh(I) and the Rh(III)-alkyl species exists, followed by the formation of the Rh(III)-acyl species as the final product.



Scheme 1

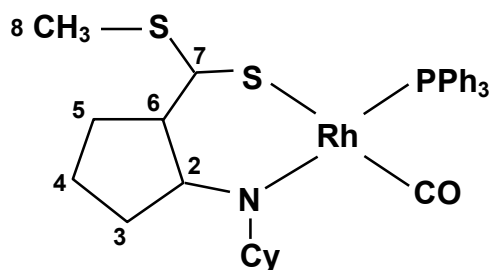
This paper describes the manipulation of the electron density on the central metal atom of $[\text{Rh}(\text{N,S-BID})(\text{CO})(\text{PX}_3)]$ complexes by introduction of different monodentate phosphine ligands PX_3 {where X = phenyl (*Ph*), *para*-chlorophenyl (*p-Cl-Ph*), *para*-methoxyphenyl (*p-MeO-Ph*) and cyclohexyl (*Cy*)} and introducing the methyl 2-(cyclohexylamino)-1-cyclopentene 1-dithiocarboxylato ligand (*cacsm*) wherein the nitrogen atom on the bidentate ligand is functionalised by a cyclohexyl group. The introduction of the bulky *Cy*-substituent improved the long-term stability of the $[\text{Rh}(\text{N,S-BID})(\text{CO})(\text{PX}_3)]$ complex, and enabled the evaluation of the thermodynamic stability of the intermediate alkyl complex (Scheme 1). The solvent effect on the above reaction was also investigated and the crystal structure of the title complex was determined.

2. Experimental

2.1. General

All the chemicals used were of reagent grade and all preparations and measurements were carried out in air. Infrared spectra were recorded on a Hitachi 270-50 instrument in KBr disks or in NaCl cells, and visible absorption spectra on Hitachi 150-20 and GBC-

916-UV spectrophotometers. The methyl ester of 2-(cyclohexylamino)-1-cyclopentene-2-dithiocarboxylic acid (cacsmH) was prepared as described earlier.⁶ ¹H NMR spectra were recorded on a Bruker 300 MHz spectrometer and were referenced relative to solvent peaks. NMR data are reported for the cacsm ligand as indicated below. ³¹P NMR spectra were recorded in CDCl₃ at 121.497 MHz relative to 85% H₃PO₄.



2.2. Preparation of complexes

(Methyl 2-(cyclohexylamino)-1-cyclopentene-1-dithiocarboxylato-κN-κS)dicarbonyl rhodium(I), [Rh(cacsm)(CO)₂]

CacsmH (0.040 g, 0.16 mmol) and anhydrous sodium acetate (0.035 g, 0.42 mmol) were dissolved in ca. 1.5 mL DMF at 5 °C. To this solution was added [Rh₂Cl₂(CO)₄] (0.030 g, 0.077 mmol) and the orange product was precipitated by the dropwise addition of a minimum ice cold water. The solid product was filtered on a sintered glass funnel and quickly re-dissolved in acetone (ca. 2 mL) for further synthetic use. Yield: 0.026 g (>40%). IR (ν(CO), cm⁻¹): (KBr): 2056(s), 1992(s).

[Rh(cacsm)(CO)(PPh₃)] (1a)

To the above mentioned solution (ca. 2 mL) containing [Rh(cacsm)(CO)₂] was added solid PPh₃ (0.042 g, 0.16 mmol) and the [Rh(cacsm)(CO)(PPh₃)] complex precipitated after scratching the bottom of the beaker with a small spatula. The complex was filtered (yield: 0.034 g; 84%). Crystals suitable for X-ray structure determination (covered with a thin layer of Canada balsam to avoid losing the solvent acetone) were obtained from more dilute acetone solutions at 0 °C after 2-3 h. IR (ν(CO), cm⁻¹): (KBr): 1944(s). (CHCl₃): 1994(s). ¹H NMR (C₆D₆): δ(ppm) 1.22, 1.52, 1.79, 2.05, 2.71, 3.45: (6×m, 11×H, N-C₆H₁₁); 2.17: (s, 3×H, S-CH₃); 2.18: (t, 2×H, -CH₂₍₃₎); 1.34: (m, 2×H, -CH₂₍₄₎);

2.77: (t, 2×H, -CH₂₍₅₎); 7.01: (m, 9×H, 2×(o-H-Ph)₃ + 1×(p-H-Ph)₃); 7.92: (m, 6×H, 2×(m-H-Ph)₃). ³¹P NMR (CDCl₃) δ(ppm): 47.4; ¹J(P-Rh) 144.6 Hz.

[Rh(cacsm)(CO)(PX₃)], (X = *p*-Cl-Ph or *p*-MeO-Ph or Cy)

These complexes were prepared as described for the [Rh(cacsm)(CO)(PPh₃)] complex in the previous paragraph. IR (KBr, cm⁻¹); ν(CO); X = *p*-Cl-Ph, 1962(s); X = *p*-MeO-Ph, 1956(s); X = Cy, 1929(s).

[Rh(cacsm)(CO)(P(p-Cl-Ph)₃)] (**1b**)

¹H NMR (C₆D₆): δ(ppm) 1.25, 1.55, 1.81, 2.04, 2.65, 3.43 (6×m, 11×H, N-C₆H₁₁); 2.14: (s, 3×H, S-CH₃); 2.16: (t, 2×H, -CH₂₍₃₎); 1.40: (m, 2×H, -CH₂₍₄₎); 2.74: (t, 2×H, -CH₂₍₅₎); 7.10 (6×H) and 7.54(6×H): (2×m, 12×H, 2×(m-H-Ph)₃ + 2×(o-H-Ph)₃). ³¹P NMR (CDCl₃) δ(ppm): 45.7; ¹J(P-Rh) 147.1 Hz.

[Rh(cacsm)(CO)(P(p-MeO-Ph)₃)] (**1c**)

¹H NMR (C₆D₆): δ(ppm) 1.29, 1.55, 1.83, 2.11, 2.81: (5×m, 11×H, N-C₆H₁₁); 2.27: (s, 3×H, S-CH₃); 2.23: (t, 2×H, -CH₂₍₃₎); 1.37: (m, 2×H, -CH₂₍₄₎); 2.82: (t, 2×H, -CH₂₍₅₎); 6.72(6×H) and 7.94(6×H): (2×m, 12×H, 2×(m-H-Ph)₃ + 2×(o-H-Ph)₃). ³¹P NMR (CDCl₃) δ(ppm): 41.5; ¹J(P-Rh) 146.1 Hz.

[Rh(cacsm)(CO)(P(Cy)₃)] (**1d**)

¹H NMR (C₆D₆): δ(ppm), 1.40, 1.58, 1.83, 2.02, 2.44: (5×m, 11×H, N-C₆H₁₁); 2.66: (s, 3×H, S-CH₃); 2.14: (t, 2×H, -CH₂₍₃₎); 1.29: (m, 2×H, -CH₂₍₄₎); 2.78: (t, 2×H, -CH₂₍₅₎); 1.20, 1.72, 2.15, 2.70: (4×wp, 33H, 3×(C₆H₁₁)).

Iodomethyl(methyl 2-(cyclohexylamino)-1-cyclopentene-1-dithiocarboxylato-κN-κS)carbonyl(tri-X-phosphine)rhodium(III). *[Rh(I)(cacsm)(CH₃)(CO)-(PX₃)]* (**2**)

The intermediate alkyl complexes (**2**) (forming within seconds and converting to the acetyl species (**3**) within minutes) were characterised in solution by ¹H and ³¹P NMR, and IR spectroscopy, as shown previously.³ Data for X=Ph (**2a**): IR (ν(CO), cm⁻¹):

(CHCl₃, cm⁻¹): 2050. ¹H NMR (C₆D₆): δ(ppm) 1.20, 1.51, 1.71, 2.00, 2.70, 3.44: (6×m, 11×H, N-C₆H₁₁); 1.10 (t, 3×H, Rh-CH₃, {²J(RhCH)~³J(PRhCH)~2Hz}) 2.06: (s, 3×H, S-CH₃); 2.09: (t, 2×H, -CH₂₍₃₎); 1.30: (m, 2×H, -CH₂₍₄₎); 2.73: (t, 2×H, -CH₂₍₅₎); 7.3-7.9: (m, 15×H, -Ph₃). ³¹P NMR (CDCl₃) δ(ppm): 29.3; ¹J(P-Rh) 128 Hz. X=*p*-Cl-Ph (**2b**): ³¹P NMR (CDCl₃) δ(ppm): 27.5; ¹J(P-Rh) 127 Hz. X= *p*-MeO-Ph (**2c**): ³¹P NMR (CDCl₃) δ(ppm): 41.5; ¹J(P-Rh) 146.1 Hz.

Acetyliodo(methyl 2-(cyclohexylamino)-1-cyclopentene-1-dithiocarboxylato-κN-κS)(tri-X-phosphine)rhodium(III). [Rh(I)(cacsm)(COCH₃)(PX₃)] (X = Ph, *p*-Cl-Ph or *p*-MeO-Ph or Cy)

The acetyl complexes (**3**) are the final products in Scheme 1 and complexes of this type have been characterised by X-ray crystallography and other methods.⁴ To a saturated benzene solution of [Rh(cacsm)(CO)(PPh₃)] (2 mL) was added 3 drops of iodomethane. After 20 min, the solution was cooled to 2 °C and slow evaporation of the solvent overnight yielded red, excessively twinned crystals (0.020 g, yield >70%)⁷.

Data for X=Ph (**3a**): IR (ν(CO), cm⁻¹): (CHCl₃): 1714; (KBr): 1712. ¹H NMR (C₆D₆): δ(ppm) 1.24, 1.58, 1.73, 1.98, 2.71, 3.45: (6×m, 11×H, N-C₆H₁₁); 2.10: (s, 3×H, S-CH₃); 2.12: (t, 2×H, -CH₂₍₃₎); 1.30: (m, 2×H, -CH₂₍₄₎); 2.72: (t, 2×H, -CH₂₍₅₎); 2.15: (s, 3×H, COCH₃); 7.2-7.8: (m, 15×H, 3×Ph). ³¹P NMR (CDCl₃) δ(ppm): 27.3; ¹J(P-Rh) 121 Hz.

Data for X= *p*-Cl-Ph (**3b**): IR (ν(CO), cm⁻¹): (CHCl₃): 1713. ³¹P NMR (CDCl₃) δ(ppm): 26.5; ¹J(P-Rh) 120 Hz. X= *p*-MeO-Ph (**3c**): IR (ν(CO), cm⁻¹): (CHCl₃): 1714. ³¹P NMR (CDCl₃) δ(ppm): 41.5; ¹J(P-Rh) 146.1 Hz.

2.3. Kinetic Measurements

The two reaction steps shown in Scheme 1 could be monitored by UV/visible measurements for all complexes, except for the [Rh(cacsm)(CO)(PCy₃)] complex, where only one reaction was observed. More rapid first reactions (as in the case of [Rh(cacsm)(CO)(PPh₃)] and [Rh(cacsm)(CO)(P(*p*-MeO-Ph)₃)]) were monitored on a Durrum D110 stopped-flow instrument or, in the case of the slower reactions, on a GBC-916 UV-visible spectrophotometer. Control kinetic experiments utilising IR (NaCl cells), ¹H and ³¹P NMR spectroscopy were done for every complex to confirm the reaction

progress as monitored by the UV-visible studies, and the rates obtained from the three methods did not differ significantly. All temperatures are reported to ± 0.1 °C accuracy. The observed first-order rate constants were calculated from absorbance vs. time data for both the fast and slow reactions by means of the least-squares program SCIENTIST.⁸ All reactions were monitored under pseudo-first-order conditions with $[\text{Rh}] = 1.5\text{-}5 \times 10^{-4}$ M. Variation of $[\text{Rh}]$ by this factor of ca. four showed no influence on the rate constants. Different selected kinetic runs under nitrogen atmosphere showed no appreciable affect on the rates and reaction yields and the kinetics were consequently studied under normal laboratory conditions. The kinetics of all the complexes were investigated in chloroform (freshly distilled) and acetone as solvents while the kinetics of $[\text{Rh}(\text{cacs m})(\text{CO})(\text{P}(p\text{-MeO-Ph})_3)]$ was also studied in ethyl acetate. Supplementary material of rate constants is available from the authors.

2.4. Structure determination

The three dimensional intensity data (MoK_α radiation) were collected on a Syntex P-1 Diffractometer. All reflections were corrected for Lorentz and polarization effects, while data reduction was performed by the PROFIT program.⁹ The structure was solved by the Patterson method (SHELXS86¹⁰) and successive Fourier syntheses (SHELXL97¹¹). All the relevant structural detail and refinement parameters are given in Table 1. The hydrogen atom positions were calculated using a riding model [phenyl C-H = 0.92 Å; methylene C-H = 0.97 Å; methyl C-H = 1.08 Å],¹¹ and were refined with an overall isotropic thermal parameter. Complete sets of structure factors, anisotropic thermal parameters and hydrogen atomic coordinates are available as Supplementary Material.

Table 1 Crystallographic data for $[\text{Rh}(\text{cacs m})(\text{CO})(\text{PPh}_3)] \cdot \text{CH}_3\text{COCH}_3$ (**1**).

Formula	$\text{C}_{35}\text{H}_{41}\text{NS}_2\text{O}_2\text{PRh}$
Formula weight	705.7
Crystal system	Triclinic
Space group	$P\bar{1}$
a /Å	9.856(2)
b /Å	11.008(2)
c /Å	16.407(3)
α /°	94.40(2)

Table 1 (cont.) Crystallographic data for [Rh(cacsm)(CO)(PPh₃)]·CH₃COCH₃ (**1**).

$\beta / ^\circ$	82.72(2)
$\gamma / ^\circ$	103.39(3)
$V / \text{\AA}^3$	1715.7(6)
Z	2
$\rho_{\text{calc}} / \text{Mg m}^{-3}$	1.366
Crystal dimensions /mm	0.40×0.25×0.15
$F(000)$	732
Diffractometer	SYNTEX P-1
Radiation /graphite monochromated; λ	Mo K α ; 0.70173 \AA
μ / mm^{-1}	0.697
Scan type	θ - 2θ
θ limits / $^\circ$	1.9- 25.1
Octants collected	$\pm 11; \pm 13; +19$
Number of data collected	6410
Number of unique data used	5059
Number of variables	389
Decay	<1%
R_1 ^{a)}	0.045
wR_2 ^{b)}	0.106
Goodness of fit	1.166
Residual electron density /max/min/	0.63/-0.64

a) $R_1 = \sum ||F_o| - |F_c|| / |F_o|$

b) Ref 11, $wR_2 = \{ \sum [w(F_o^2 - F_c^2)^2] / \sum [w(F_o^2)^2] \}^{0.5}$; Weighting scheme: $w = 1 / [\sigma^2(F_o^2) + (0.44P)^2 + 3.8P]$;
 $P = [2F_c^2 + \max(F_o^2, 0)] / 3$

3. Results and Discussion

3.1. Structure

The atom numbering of the [Rh(cacsm)(CO)(PPh₃)] molecule is given in Fig. 1 with the most important bond lengths and angles reported in Table 2. The compound crystallizes as approximately square planar [Rh(cacsm)(CO)(PPh₃)] complexes and acetone solvent molecules. The acetone molecule is ordered but has high thermal motion. It exhibits only weak van der Waals interactions of 2.6-2.8 \AA between the acetone-oxygen (O2) and the outer PPh₃-protons (H23 and H24), as well as 2.80 \AA between the carbonyl-oxygen (O1) and one acetone-methyl proton (H511).

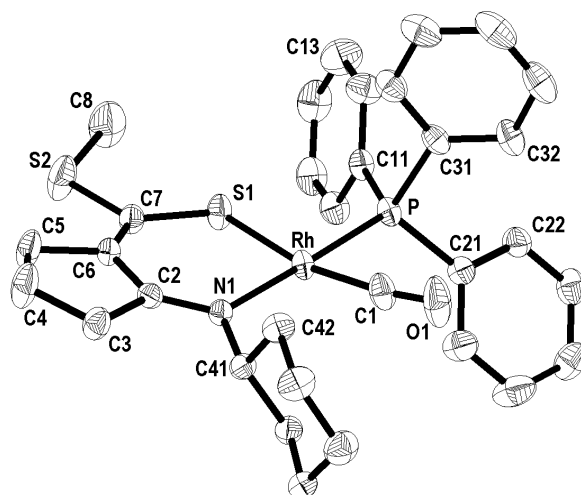


Figure 1 Atom numbering scheme for $[\text{Rh}(\text{cacsm})(\text{CO})(\text{PPh}_3)]$ (30% probability ellipsoids), with hydrogen atoms omitted for clarity. First and second digits denote ring number and atom in ring respectively.

Table 2 Selected interatomic bond distances (Å) and angles ($^\circ$) with esd's in parentheses for $[\text{Rh}(\text{cacsm})(\text{CO})(\text{PPh}_3)] \cdot \text{CH}_3\text{COCH}_3$.

Rh-C(1)	1.828(5)	S(2)-C(7)	1.770(5)
Rh-N(1)	2.125(3)	C(1)-O(1)	1.155(6)
Rh-P	2.2681(12)	C(7)-C(6)	1.349(6)
Rh-S(1)	2.2917(14)	C(6)-C(2)	1.434(6)
P-C(11)	1.836(5)	C(6)-C(5)	1.518(6)
P-C(31)	1.832(5)	C(3)-C(4)	1.502(7)
N(1)-C(2)	1.316(5)	C(3)-C(2)	1.535(6)
N(1)-C(41)	1.495(5)	C(4)-C(5)	1.455(8)
S(1)-C(7)	1.710(5)	C(41)-C(46)	1.514(6)
S(2)-C(8)	1.772(7)	C(41)-C(42)	1.525(6)
C(1)-Rh-N(1)	97.8(2)	C(12)-C(11)-P	123.8(4)
C(1)-Rh-P	83.0(2)	N(1)-C(41)-C(46)	113.6(4)
N(1)-Rh-P	178.5(1)	N(1)-C(41)-C(42)	111.8(4)
C(1)-Rh-S(1)	167.5(2)	C(46)-C(41)-C(42)	112.6(4)
N(1)-Rh-S(1)	93.5(1)	O(1)-C(1)-Rh	171.6(5)
P-Rh-S(1)	85.55(5)	C(6)-C(7)-S(1)	128.2(4)
C(21)-P-C(11)	99.6(2)	C(6)-C(7)-S(2)	115.8(3)
C(21)-P-C(31)	105.8(2)	S(1)-C(7)-S(2)	116.1(3)
C(11)-P-C(31)	104.0(2)	C(7)-C(6)-C(2)	128.8(4)
C(21)-P-Rh	117.3(2)	C(7)-C(6)-C(5)	121.3(4)
C(11)-P-Rh	119.7(2)	C(2)-C(6)-C(5)	109.8(4)
C(31)-P-Rh	108.8(2)	C(4)-C(3)-C(2)	105.9(4)
C(2)-N(1)-C(41)	114.3(4)	N(1)-C(2)-C(6)	129.4(4)
C(2)-N(1)-Rh	126.7(3)	N(1)-C(2)-C(3)	123.2(4)
C(41)-N(1)-Rh	118.8(3)	C(6)-C(2)-C(3)	107.4(4)
C(7)-S(1)-Rh	111.7(2)	C(5)-C(4)-C(3)	109.1(4)
C(8)-S(2)-C(7)	106.6(3)	C(4)-C(5)-C(6)	106.5(4)

Only one carbonyl ligand is substituted when reacting $[\text{Rh}(\text{cacsm})(\text{CO})_2]$ with PPh_3 to form the $[\text{Rh}(\text{cacsm})(\text{CO})(\text{PPh}_3)]$ complex, which is in agreement with what was found in previous studies.⁴ Although it is expected that the carbonyl *trans* to the sulfur atom should be substituted by PPh_3 in the $[\text{Rh}(\text{N,S-BID})(\text{CO})_2]$ complex, the reactivity of the Rh(I) center is such that the thermodynamically stable isomer will be favoured in solution after a short time. The thermodynamically stable isomer in solution and that characterised by X-ray crystallography was the one with the *trans* N-Rh-P orientation, similar to that found in $[\text{Rh}(\text{macsm})(\text{CO})(\text{PPh}_3)]$ ⁴ $\text{macsm} = (\text{methyl } 2\text{-}(\text{methylamino})\text{-}1\text{-cyclopentene-}1\text{-dithiocarboxylate})$. It is known^{12,13} that it is not necessarily always the thermodynamically stable isomer that crystallises out since the crystallisation energy of a specific isomer will determine the solid state structure, specifically in labile Rh(I) systems.

The observed Rh-P bond length of 2.268(1) Å obtained from this study is in excellent agreement with the Rh-P bond distances of 2.258(2)-2.281(2) Å found in previous studies for the same type of $[\text{Rh}(\text{BID})(\text{CO})(\text{PPh}_3)]$ complexes. In these the PPh_3 was also *trans* to a coordinating nitrogen atom in six- and five-membered chelate rings formed between the bidentate ligand and the Rh atom^{14,15} and is almost identical to the 2.269(1) Å found in the $[\text{Rh}(\text{macsm})(\text{CO})(\text{PPh}_3)]$ complex.³

It is interesting to note the significant increase in the Rh-N bond length of 2.125(3) Å compared with those previously found where the nitrogen atom was also positioned *trans* to PPh_3 in the related $[\text{Rh}(\text{BID})(\text{CO})(\text{PPh}_3)]$ complexes, *i.e.*, 2.088(6), 2.092(7), 2.098(9) and 2.087(4) Å for BID = 2-picolinate,¹⁶ N-*o*-tolylsalicylaldiminate,¹⁷ 8-hydroxyquinolate¹⁸ and methyl 2-(methylamino)-1-cyclopentene 1-dithiocarboxylate³ respectively. The steric interaction between the bulky cyclohexyl group on the nitrogen atom and the carbonyl ligand causes the *cacsm* ligand to rotate away from the carbonyl (yet still in the square planar plane) on the nitrogen side of the ligand and towards the phosphine on the sulfur side, and forced the carbonyl upwards. This is illustrated by the out of plane bending of the Rh-CO bond ($\text{S}(1)\text{-Rh-C}(1) = 167.5(2)^\circ$). Further manifestation of this fact comes from the shorter Rh-S bond distance of 2.292(1) Å, compared with the equivalent bond distance of 2.298(1) Å in $[\text{Rh}(\text{macsm})(\text{CO})(\text{PPh}_3)]$. This shift of the N,S-BID-ligand within the square plane is also observed in the

respective decrease and increase of the S-Rh-P and N-Rh-C(1) bond angles (85.6(1) and 97.8(2)°) compared with the equivalent angles of 87.5(1) and 94.1(2)° in [Rh(macsm)(CO)(PPh₃)]. The net result of the large steric demand of the cyclohexyl group (vs. the methyl in the macsm complex) is therefore that the complete N-S bidentate backbone is "rotated" by ca. 2-3° in the plane, away from the Rh-CO bond towards the direction of the Rh-P bond. This intramolecular steric repulsion is also manifested in the subtle distortion in the PPh₃ ligand, as is clear from (i) the Rh-P-C(11) and Rh-P-C(12) bond angles (119.7(2) and 117.3(2) °), compared to the Rh-P-C(13) angle of 108.8(2) °, and (ii) the C(11)-P-C(12) (99.6(2) °, compared with the C(11)-P-C(13) and C(12)-P-C(13) angles of 104.0(2) and 105.8(2) °, respectively. The dihedral angle between the planes formed by the Rh-coordinated atoms and those forming the chelate ring is 12.5(2)°, which is substantially larger than the ca. 3° observed in the corresponding [Rh(macsm)(CO)(PPh₃)] complex,³ again indicative of intramolecular strain as pointed out above.

The Rh-CO bond length of 1.828(5) Å is comparable with the bond length of 1.836(5) Å found in the [Rh(macsm)(CO)(PPh₃)] complex³ wherein the carbonyl ligand is also coordinated *trans* to a sulfur donor atom. Both these bond lengths are significantly longer than in similar complexes where the carbonyl was *trans* to an oxygen atom in similar [Rh(BID)(CO)(PPh₃)] complexes; the average Rh-CO distance in fourteen of these was 1.796(8) Å.^{14-18,19, 20, 21} The Rh-CO bond length increase can be ascribed directly to the large *trans* influence of sulfur, increasing the nucleophilicity of the metal center and thus effectively decreasing the σ-donating ability of the CO-ligand, resulting in a weaker Rh-CO bond.

Upon comparison of the bond lengths in the chelate ring, that is N-C(2)-C(6)-C(7)-S(1), 1.315(5), 1.434(6), 1.349(6), 1.710(5) Å, with the respective single bond distances N-C(41), 1.495(5) Å; C(2)-C(3)-C(4)-C(5)-C(6), 1.455(8)-1.535(6) Å and S(2)-C(8) or S(2)-C(7), 1.772(6) Å (average), the definite shortening of all the bonds of the chelate ring is obvious. This is especially true for the C(2)-C(6), C(6)-C(7) and C(3)-C(4) bonds, clearly exhibiting significant π-character. It is also further manifested by the dihedral angle between the cyclopentene ring and the metal chelating atoms, which is only 3.3(3)°, indicative of the delocalized π-character in the chelate ring bonds.

A general decrease of $\nu(\text{CO})$ in the $[\text{Rh}(\text{cacs})\text{m}(\text{CO})(\text{PX}_3)]$ complexes as the basicity of the tertiary phosphines increases, was observed: $X=(p\text{-Cl-Ph})$, $\nu(\text{CO})=1962$; $X=(p\text{-MeO-Ph})$, $\nu(\text{CO})=1956$; $X=(\text{Ph})$, $\nu(\text{CO})=1944$; $X=(\text{Cy})$, $\nu(\text{CO})=1929 \text{ cm}^{-1}$. It was expected that the $\nu(\text{CO})$ values for $X=(p\text{-MeO-Ph})$ and $X=(\text{Ph})$ would be the other way around, ($\text{p}K_{\text{a}}$ values of the phosphines are 1.0, 2.73, 4.57 and 9.7 for $X=p\text{-Cl-Ph}$, Ph , $p\text{-MeO-Ph}$ and Cy respectively²²). An interesting observation related to the infrared data stems from the substantial distortion induced on the $\text{Rh-C}\equiv\text{O}$ bond, which is only $171.6(5)^\circ$ and deviates significantly from linearity. It was previously shown that in the $\text{Rh}(\text{I})$ analogue of Vaska's complex,²³ *trans*- $[\text{Rh}(\text{PPh}_3)_2(\text{CO})(\text{Cl})]$, a decrease in $\nu(\text{CO})$ of 18 cm^{-1} (from 1983 to 1965 cm^{-1}) was induced by packing effects, resulting in a bending of the $\text{Rh-C}\equiv\text{O}$ bond of about 10° . This was also described in the $[\text{Rh}(\text{acac})(\text{CO})(\text{PFcPh}_2)]$ (Fc =ferrocenyl) complex where the $\text{Rh-C}\equiv\text{O}$ bond angle was found to be $170(1)^\circ$.²⁴

3.2. Kinetics

It is known for these $[\text{Rh}(\text{BID})(\text{CO})(\text{PPh}_3)]$ complexes, that in the cases where BID = unsymmetrical bidentate ligands, different isomers exist in solution.²⁵ This is specifically true for bidentate ligands with donor atoms that have similar characteristics, such as trifluoroacetylacetonate, cupferrate and aminovinylketonate chelates. In this current study, however, only minor amounts (0-5%) of the thermodynamically unstable isomers (*i.e.* for the complexes $[\text{Rh}(\text{cacs})\text{m}(\text{CO})(\text{PX}_3)]$) with *trans* S-Rh-P moieties were observed. Since these thermodynamically unfavourable isomers were present in such low concentrations for all the complexes investigated in this study, possible interference therefrom was ignored.

The reaction progress of the iodomethane oxidative addition to $[\text{Rh}(\text{cacs})\text{m}(\text{CO})(\text{P}(p\text{-MeO-Ph}))]$ is shown in Fig. 2. At large $[\text{MeI}]$ ((b) in Fig. 2) the formation of the alkyl intermediate (band at 2080 cm^{-1}) is well defined, which then converts to the acyl species (band at 1713 cm^{-1}). However, at lower $[\text{MeI}]$, as illustrated in (a), the alkyl intermediate band at 2080 cm^{-1} is not so pronounced, and the disappearance of the $\text{Rh}(\text{I})$ at 1960 cm^{-1} is virtually identical to the formation of the acyl species. These spectral changes clearly indicate a mechanism as shown in Scheme 1,

typical of a rapid pre-equilibrium followed by a relatively slow acyl formation, for which the rate expressions are given in Eqs. 1 and 2 as discussed below. In all the reactions studied, there was no indication of an equilibrium for the formation of the acyl species. Thus, in Scheme 1, $k_{-2} = 0$.

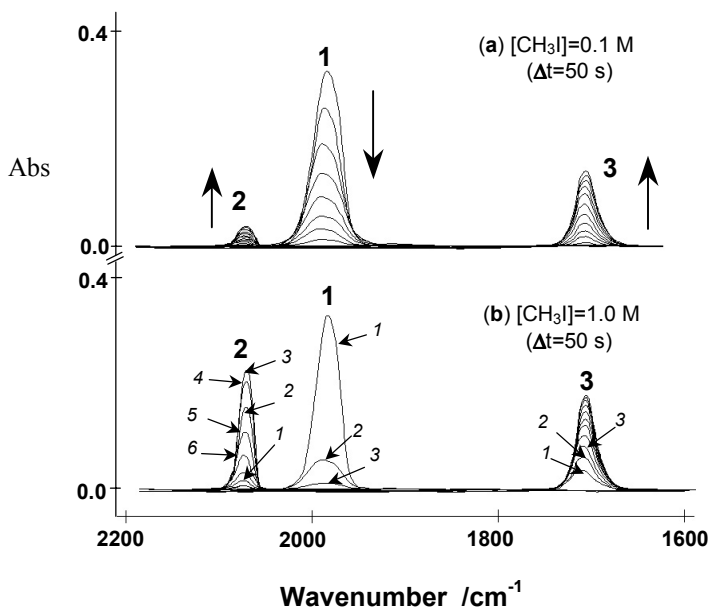


Figure 2 Repetitive IR scans for $[\text{Rh}(\text{cacs})\text{m}(\text{CO})(\text{P}(p\text{-MeO-Ph})_3)]$; CHCl_3 , $25\text{ }^\circ\text{C}$, $[\text{Rh}]_{\text{tot}} = 1.6 \times 10^{-4}\text{ M}$: (a) $[\text{CH}_3\text{I}] = 0.1\text{ M}$; (b) $[\text{CH}_3\text{I}] = 1.0\text{ M}$ [See also scheme 1: **1** Rh(I)-reactant, **2** Rh(III)-alkyl, **3** Rh(III)-acyl].

The starting complexes could be adequately characterised by ^1H NMR spectroscopy. However, the ^1H spectra of the intermediate alkyl and acyl species were quite complex due to the non-equivalence introduced at the protons on the cyclopentene and cyclohexyl moieties. All the complexes could however be characterised by ^{31}P NMR spectroscopy.

It is interesting to note that the overall reaction proceeds from a square planar (classic sixteen electron complex) via the intermediate octahedral eighteen electron species to eventually form the five-coordinate, square pyramidal moiety (classic sixteen electron complex).⁴

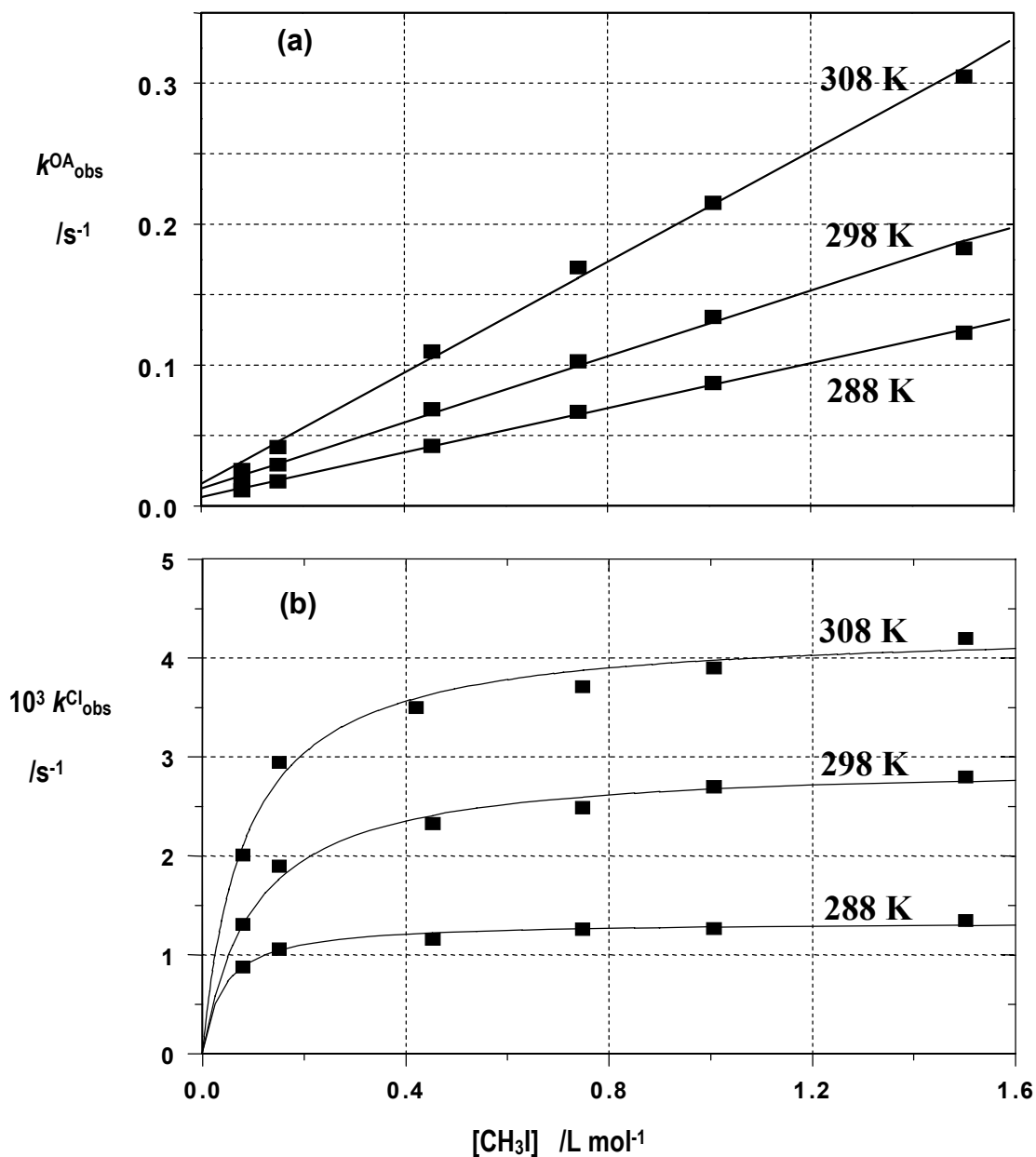


Figure 3 Temperature and $[CH_3I]$ dependence of the pseudo-first-order rate constant for the formation of (a) $[Rh(I)(cacsm)(CO)(P(p-MeO-Ph)_3)(CH_3)]$ (alkyl product, Scheme 1); (b) $[Rh(I)(cacsm)(COCH_3)(P(p-MeO-Ph)_3)]$ (acyl product, Scheme 1) in $CHCl_3$, $[Rh]_{tot} = 1.6 \times 10^{-4}$ M.

A plot of the observed first-order rate constants of the oxidative addition reaction (step I in Scheme 1) vs. iodomethane concentration, yields a linear relationship with a non-zero intercept for $P(p-Cl-Ph)_3$, PPh_3 and $P(p-MeO-Ph)_3$ as phosphine ligands in the metal complex. An example of such a plot is shown in Fig. 3(a), in which the solid lines

represent the least-squares fits of the $k_{\text{obs}}^{\text{OA}}$ -data vs. $[\text{CH}_3\text{I}]$ to Eq. 1 (at three different temperatures). This is consistent with the rate expression of an equilibrium reaction as presented as the first step in Scheme 1, with $k_{\text{obs}}^{\text{OA}}$ = pseudo first order rate constant for the oxidative addition step. The respective k_1 and k_{-1} constants are given in Table 3.

$$k_{\text{obs}}^{\text{OA}} = k_1[\text{CH}_3\text{I}] + k_{-1} \quad (1)$$

Table 3 Kinetic and equilibrium data for the oxidative addition of iodomethane to complexes of the type $[\text{Rh}(\text{N,S-BID})(\text{CO})(\text{PX}_3)]$ (N,S-BID=cacsm, macsm, macsh respectively) in different solvents at 25 °C.

N,S-BID and Solvent	$\epsilon, D_n^{\text{a)}$	$X^{\text{b)}$	$10^3 k_1$ /L mol ⁻¹ s ⁻¹	$10^3 k_{-1}$ /s ⁻¹	$\Delta H^\ddagger(k_1)$ /kJ mol ⁻¹	$\Delta S^\ddagger(k_1)$ /J K ⁻¹ mol ⁻¹	$K_1^{\text{c)}$ /L mol ⁻¹	$K_1^{\text{d)}$ /L mol ⁻¹	$10^3 k_2$ /s ⁻¹
<u>cacsm</u>									
chloroform	5; 4	<i>p</i> -MeO-Ph	117(4)	12(3)	38(7)	-134(20)	10(2)	12(2)	2.9(1)
acetone	21; 17	<i>p</i> -MeO-Ph	108(4)	15(3)	--	--	7.2(4)	4(1)	9.4(3)
ethyl acetate	6; 17	<i>p</i> -MeO-Ph	25(5)	15(4)	--	--	1.6(4)	0.8(3)	17(1)
chloroform	5; 4	Ph	56(1)	19(1)	39(7)	-138(20)	2.9(1)	3(1)	5(1)
acetone	21; 17	Ph	43(5)	11(3)	--	--	4(1)	--	--
chloroform	5; 4	<i>p</i> -Cl-Ph	10(1)	8(1)	25(5)	-192(16)	1.3(3)	1.1(3)	6.2(8)
acetone	21; 17	<i>p</i> -Cl-Ph	20(1)	2.7(3)	--	--	7.3(6)	--	--
chloroform	5; 4	Cy	0.2 ^{e)}	2 ^{e)}	54(1) ^{f)}	-122(4) ^{f)}	0.1	--	7 ^{e)}
<u>macsh</u> ^{g)}									
chloroform	5; 4	Ph	380(1)	26(4)	26(4)	-166(13)	15(3)	36(4)	7.2(2)
<u>macsm</u> ^{h)}									
chloroform	5; 4	Ph	34(1)	8.6(8)	23(3)	-195(11)	4(1)	4(1)	7.6(4)

a) Ref. 28.

b) For PX_3 , Ph=Phenyl, X=*p*-MeO-Ph=*para*methoxyphenyl, *p*-Cl-Ph=*para*chlorophenyl, Cy=cyclohexyl.

c) $K_1 = k_1/k_{-1}$; Eq.1.

d) Eq. 2.

e) Estimated from IR data, from $K_1 k_2 = 7.7(1) \times 10^{-4} \text{ s}^{-1}$ (Suppl. Material), and assuming $k_2 = 7 \times 10^{-3} \text{ s}^{-1}$.

f) Calculated for combined forward rate constant $k_2 K_1$.

g) Ref. 4; macsh=2-methylamino-1-cyclopentene-1-dithiocarboxylate.

h) Ref. 4, macsm=methyl 2-(methylamino)-1-cyclopentene-1-dithiocarboxylate.

A plot of the observed first-order rate constants vs. $[\text{CH}_3\text{I}]$ for the formation of the acyl species (step II in Scheme 1) for the complexes $[\text{Rh}(\text{cacsm})(\text{CO})(\text{P}(\textit{p}\text{-Cl-Ph})_3)]$ and $[\text{Rh}(\text{cacsm})(\text{CO})(\text{P}(\textit{p}\text{-MeO-Ph})_3)]$ shows limiting kinetics as depicted in Fig. 3(b). The solid curved lines represent the least-squares fits of the k_{obs} -data ($k_{\text{obs}}^{\text{CI}}$ = CO insertion

step) vs. $[\text{CH}_3\text{I}]$ to Eq. (2) (at three different temperatures), which corresponds to a mechanism consisting of a fast pre-equilibrium reaction as presented in Scheme 1 (K_1 = equilibrium constant), followed by a second slower reaction with a rate constant k_2 . The values obtained for K_1 and k_2 are listed in Table 3.

$$k_{\text{obs}}^{\text{Cl}} = \frac{k_2 K_1 [\text{CH}_3\text{I}]}{1 + K_1 [\text{CH}_3\text{I}]} \quad (2)$$

It is clear from Table 3 that there is an excellent agreement between the equilibrium constant for the formation of the alkyl complex as obtained from studying the first and second steps separately. This, together with the IR data as typically shown in Fig. 2, confirms the mechanism as proposed in Scheme 1. This limiting dependence is also in agreement with that previously observed for the Rh(III)-alkyl disappearance (as in $[\text{Rh}(\text{I})(\text{macsm})(\text{CO})(\text{PPh}_3)(\text{CH}_3)]^3$ and Rh(III)-acyl formation (as in $[\text{Rh}(\text{I})(\text{macsm})(\text{COCH}_3)(\text{PPh}_3)]$), for which the reaction rate constants were also equal within experimental error.

In the case of the reaction between $[\text{Rh}(\text{cacsm})(\text{CO})(\text{PCy}_3)]$ and iodomethane, however, only one step is observed by UV-visible spectroscopy, and the plot of the observed first-order rate constants vs. $[\text{CH}_3\text{I}]$ shows a linear relationship with a very small intercept. When this reaction was monitored by infrared spectroscopy, time scans between 2200 and 1650 cm^{-1} showed only a very small peak at 2050 cm^{-1} , corresponding to the intermediate Rh(III)-CO-alkyl species (Fig. 2(a)). This implies that the formation of this intermediate Rh(III)-CO-alkyl species is thermodynamically unfavourable, but that it still *does form*, albeit in small concentrations.

This was also the case in a previous study done by Botha *et al.*²¹ for the oxidative addition of iodomethane to $[\text{Rh}(\text{Sacac})(\text{CO})(\text{PX}_3)]$ (Sacac= thioacetylacetonate), where the X substituents were the same as in this current study. However, the mechanism in the latter case was presented as in Scheme 1 but with the k_{-1} path absent. It was consequently assumed that formation of the Rh(III)-acyl species was *more rapid* than that of the Rh(III)-alkyl species ($k_2 \gg k_1$), *i.e.*, that the Rh(III)-alkyl species could be considered as a steady state intermediate. However, if a small equilibrium constant (K_1) is assumed for the first equilibrium step of the mechanism presented for the reaction of

[Rh(cacsm)(CO)(PCy₃)] with iodomethane, Eq. 2 simplifies to $k_{\text{obsd}} = k_2K_1[\text{CH}_3\text{I}]$, which predicts a linear relationship between k_{obsd} and $[\text{CH}_3\text{I}]$ with the second order rate constant equal to k_2K_1 . This result confirms that the same general mechanism holds as described for the complexes where P(*p*-Cl-Ph)₃, PPh₃ and P(*p*-MeO-Ph)₃ were used as the phosphines in the metal complex. However, what is observed spectrophotometrically is finally kinetically controlled by a small K_1 value for [Rh(cacsm)(CO)(PCy₃)]. This is exactly what is to be expected considering the large steric demand of PCy₃, which inhibits the formation of the Rh(III) alkyl species.

The three tertiary phosphines P(*p*-Cl-Ph)₃, PPh₃ and P(*p*-MeO-Ph)₃ have the same cone angle θ of 145°²⁶, and will therefore have virtually the same steric demand. However, electronically there is an increase in their σ -donating ability from left to right as is predicted by their Bronsted pK_a values²² of 1.03, 2.73 and 4.57, respectively. The second-order rate constants for the oxidative addition (k_1), show an order of magnitude increase from P(*p*-Cl-Ph)₃ to P(*p*-MeO-Ph)₃ (Table 3), which is in direct agreement with the higher basicity of the respective Rh(I) complexes. However, if the pK_a -value of PCy₃ (9.7) is considered, it is anticipated that k_1 should be larger compared with the other phosphines, due to the increased nucleophilicity introduced to the metal center. This is not the case, since the cone angle of PCy₃ is very large (170°²⁶) and thus has a much larger steric demand compared with the others. The latter consequently overshadows the electronic effect, resulting in an estimated second order constant of only $1.5 \times 10^{-5} \text{ L mol}^{-1} \text{ s}^{-1}$ (Table 3). This is *ca.* three orders of magnitude smaller than the rate constants observed for the other three phosphines. The [Rh(cacsm)(CO)(PCy₃)] complex is thus significantly deactivated towards iodomethane oxidative addition.

Furthermore, the influence of the reverse path (k_{-1}) must also be taken into account, since it is possible that PCy₃ will also *increase* the value of k_{-1} , *i.e.*, favour reductive elimination, compared with less sterically demanding phosphines such as the *p*-substituted phenyl moieties employed in this study. Already arguing a smaller $K_1 = k_1/k_{-1}$ value for the reaction between [Rh(cacsm)(CO)(PCy₃)] complex and iodomethane, the latter argument supports the previous one, that the oxidative addition of iodomethane to the [Rh(cacsm)(CO)(PCy₃)] complex proceeds according to the

mechanism presented in Scheme 1, with the special case where K_1 is small (controlled by a *smaller* k_1 and a *larger* k_{-1} value).

The effect of increased basicity on the reverse path (k_{-1}) introduced to the metal center by the phosphine ligand is illustrated in Table 3, where a slight increase is observed from $P(p\text{-Cl-Ph})_3$ to $P(p\text{-MeO-Ph})_3$ (25 °C). Again, this is in agreement with the fact that a decrease in the nucleophilicity of the rhodium center should favour reductive elimination.

Upon comparison of the iodomethane oxidative addition rate to $[\text{Rh}(\text{macsm})(\text{CO})(\text{PPh}_3)]$, ($k_1 = 0.034 \text{ L mol}^{-1} \text{ s}^{-1}$; 25 °C),³ the effect of the cyclohexyl group (compared with methyl) on the nitrogen atom for the current $[\text{Rh}(\text{cacsm})(\text{CO})(\text{PPh}_3)]$ complex, is that only a small increase in the rate ($k_1 = 0.056(1) \text{ L mol}^{-1} \text{ s}^{-1}$) is observed. This is attributed to the larger steric demand of the cyclohexyl compared to the methyl group, inhibiting the ease of the MeI moiety entering into the rhodium coordination sphere.

If the carbonyl insertion reactions (k_2 rate constants) for $P(p\text{-Cl-Ph})_3$, PPh_3 and $P(p\text{-MeO-Ph})_3$ are considered, a tendency that k_2 decreases slightly with increasing basicity of the metal complex is observed. From this tendency, it is anticipated that k_2 in the case of PCy_3 should decrease. However, the dependence of both the acyl formation and the reductive elimination steps are illustrated by the rate constant in Table 3, and indicate that the k_2 values for several of the $[\text{Rh}(\text{N,S-BID})(\text{CO})(\text{PX}_3)]$ complexes^{3,5} show a smaller *relative* effect of k_2 on the basicity of the Rh(I)-complex, compared with the more significant dependence of k_{-1} , and especially k_1 , thereon. Extrapolating this behaviour to the $[\text{Rh}(\text{cacsm})(\text{CO})(\text{PCy}_3)]$ complex and assuming k_2 to be *ca.* $5 \times 10^{-3} \text{ s}^{-1}$ at 25 °C, K_1 can be calculated as $0.15 \text{ L mol}^{-1} = k_2 K_1 / k_{-1} = (7.7 \times 10^{-4} \text{ L mol}^{-1} \text{ s}^{-1} / 5 \times 10^{-3} \text{ s}^{-1})$, which is a 1-2 order of magnitude decrease compared with the K_1 values obtained for the other complexes in this study (Table 3). The K_1 value of *ca.* 0.15 L mol^{-1} for the PCy_3 complex is thus in excellent agreement with the tendency of K_1 for all the complexes to decrease with decreasing k_1 values (Table 3).

An objective of this investigation was also to study the relative effect of electron density variation of the rhodium center on the oxidative addition rate and thermodynamic equilibria in the $[\text{Rh}(\text{cacsm})(\text{CO})(\text{PX}_3)]$ complexes. Fig. 4 illustrates the

manipulation of the rate of formation of the alkyl intermediate as manifested by the magnitude of the equilibrium constant, K_1 . It is clear that the plateau predicted by Eq. 2 can be tuned by varying the PX_3 ligand. The electron donating ability and the steric demand of the phosphine follow the same trend as the corresponding oxidative addition: $P(p\text{-MeO-Ph})_3 > PPh_3 > P(p\text{-Cl-Ph})_3 > PCy_3$, i.e., $k_1 = (1.17 \pm 0.04) \times 10^{-1}$, $(5.6 \pm 0.1) \times 10^{-2}$, $(1.0 \pm 0.1) \times 10^{-2}$, $2 \times 10^{-5} \text{ L mol}^{-1} \text{ s}^{-1}$, and $K_1: (10 \pm 2)$, (2.9 ± 0.1) , (1.3 ± 0.3) , $\sim 0.1 \text{ L mol}^{-1}$, respectively.

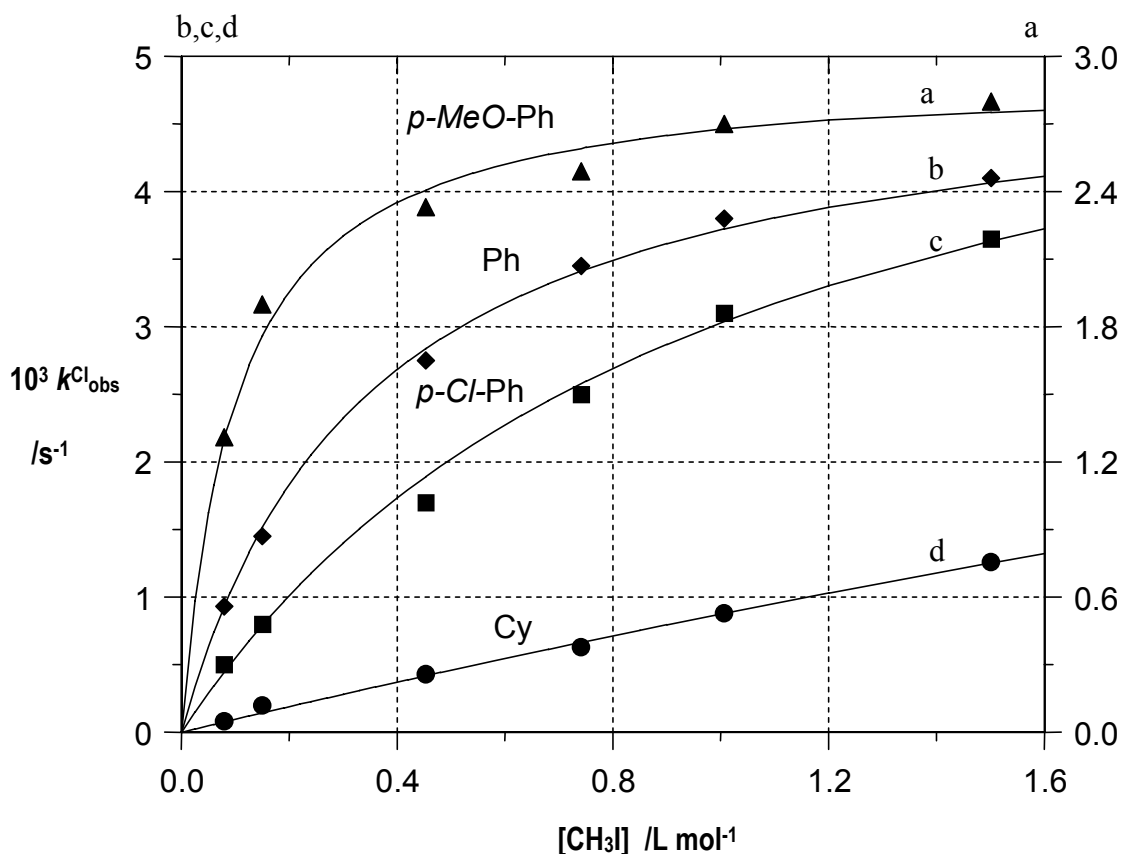


Figure 4 Effect of the X-substituent of the phosphine ligand on the kinetic and thermodynamic properties (k_1 , k_2 and K_1) vs. $[CH_3I]$ as manifested in the formation of $[Rh(I)(cacs m)(COCH_3)(PX_3)]$ (acyl product, Scheme 1) in $CHCl_3$, $[Rh]_{tot} = 1.6 \times 10^{-4} \text{ M}$, 25°C .

The activation parameters for the reaction in Scheme 1 were determined from Eyring plots and are reported in Table 3. The large negative ΔS^\ddagger -values for the oxidative addition step in chloroform for these $[Rh(N,S\text{-BID})(CO)(PX_3)]$ complexes

indicate an associative pathway for the formation of the transition state, as has been shown and discussed previously for iodomethane oxidative addition reactions in similar complexes.²⁷

In order to investigate the effect of polarity of the transition state we introduced acetone and ethyl acetate as additional solvents having similar donor ability (as defined by the donor number, D_n , or the donor strength, D_s) but different polarity (Table 3).²⁸ A 2.5 fold increase in the k_1 rate constant was observed from ethyl acetate to acetone for the oxidative addition of iodomethane to $[\text{Rh}(\text{cacs})\text{m}(\text{CO})(\text{P}(p\text{-MeO-Ph})_3)]$, but the rate constant in chloroform, although it is much less polar than acetone, did not show an appreciable effect. A more significant effect on the thermodynamics of the oxidative addition step was observed, which was stabilized in the three solvents in the order: $\text{CHCl}_3 > \text{acetone} > \text{ethyl acetate}$, *i.e.*: K_1 : (10±2), (7.2±0.4), (1.6±0.4), L mol^{-1} , respectively. This again, however, is not in agreement with the order of the polarity / donicity of these solvents.

Acknowledgement

Financial assistance by the South African NRF and the Research Fund of the University of the Free State is gratefully acknowledged. Dr. S. Otto is thanked for experimental assistance.

References

- 1 P. Maitlis, A. Haynes, G.A. Sunley and M.J. Howard, *J. Chem. Soc., Dalton Trans*, 1996, 2187.
- 2 W.A. Herrmann, *Applied Homogeneous Catalysis with Organometallic Compounds* (B. Cornils and W.A. Herrmann, eds.), VCH Weinheim, 1995.
- 3 G.J.J. Steyn, A. Roodt and J.G. Leipoldt, *Inorg. Chem.*, 1992, **31**, 3477.
- 4 A. Roodt and G.J.J. Steyn, *Recent Research Developments in Inorganic Chemistry* (S.G. Pandalai, ed), Transworld Research Network, Trivandrum. 2000, **2**, pp. 1-23.
- 5 G.J.J. Steyn, A. Roodt and J.G. Leipoldt, *Rhodium Express*, 1993, **1**, 25.

- 6 (a) B. Bordas, P. Sohar, G. Matolcsy and P. Berencsi, *J. Org. Chem.*, 1972, **37**, 1727; (b) K. Nag and D.S. Joardar, *Inorg. Chim. Acta*, 1975, **14**, 133.
- 7 Structure could not be solved due to excessive twinning. Triclinic, $P\bar{1}$, $Z = 2$; $a = 9.832(1)$, $b = 9.862(1)$, $c = 16.341(2)$ Å, $\alpha = 90.54(2)$, $\beta = 94.63(2)$, $\gamma = 114.87(2)^\circ$; $\rho_c = 1.672$; $\rho_e = 1.653$ g cm⁻³.
- 8 SCIENTIST. Program for least-squares minimization. Micromath Inc., Utah, USA.
- 9 V.A. Streltsov and V.E. Zavodnik, *Kristallographia*, 1989, **34**, 1369.
- 10 G. M Sheldrick, SHELXS-86, *Acta Cryst.*, 1990, **A46**, 467.
- 11 G.M. Sheldrick, SHELXL-97, *Program for structure refinement*, University of Göttingen, 1997.
- 12 G.J.J Steyn A. Roodt, A. Poletaeva and Y.S. Varshavsky, *J. Organomet. Chem.*, 1997, **536/7**, 797.
- 13 C.H. Langford and H.B. Gray, *Ligand Substitution Processes*, Benjamin, New York, 1965.
- 14 D.E. Graham, G.J. Lamprecht, I.M. Potgieter, A. Roodt and J.G. Leipoldt, *Transition Met. Chem.*, 1991, **16**, 193.
- 15 S.S. Basson, J.G. Leipoldt, W. Purcell, G.J. Lamprecht and H. Preston, *Acta Cryst.*, 1992, **C48**, 167.
- 16 J.G. Leipoldt, G.J. Lamprecht and D.E. Graham, *Inorg. Chim. Acta*, 1985, **101**, 123.
- 17 J.G. Leipoldt, S.S. Basson, E.C. Grobler and A. Roodt, *Inorg. Chim. Acta*, 1985, **99**, 13.
- 18 J.G. Leipoldt, S.S. Basson and C.R. Dennis, *Inorg. Chim. Acta*, 1981, **50**, 121.
- 19 K.G. van Aswegen, J.G. Leipoldt, I.M. Potgieter, G.J. Lamprecht, A. Roodt and G.J. van Zyl, *Transition Met. Chem.*, 1991, **16**, 369.
- 20 (a) L.J. Botha, S.S. Basson and J.G. Leipoldt, *Inorg. Chim. Acta*, 1987, **126**, 25; (b) A. Roodt, J.G. Leipoldt, J.C. Swarts and G.J.J. Steyn, *Acta Cryst.*, 1992, **C48**, 547; (c) J.G. Leipoldt, S.S. Basson, L.D.C. Bok and T.I.A. Gerber, *Inorg. Chim. Acta*, 1978, **25**, L35.
- 21 J.G. Leipoldt, S.S. Basson and L.J. Botha, *Inorg. Chim. Acta*, 1990, **168**, 215.

- 22 *Comprehensive Coordination Chemistry* (G. Wilkinson, ed.), Pergamon Press, New York, 1987.
- 23 G. Kemp, W. Purcell and A. Roodt, *Rhodium Express*, 1996, **16**, 17.
- 24 S.Otto, A. Roodt, J.J.C. Erasmus and J.C. Swarts, *Polyhedron*, 1998, **17**, 2447.
- 25 (a) A.M. Treciak and J.J. Ziolkowski, *Inorg. Chim. Acta*, 1985, **96**, 15; (b) W. Purcell, S.S Basson, J.G. Leipoldt, A. Roodt and H. Preston, *Inorg. Chim. Acta*, 1995, **234**, 153; (c) T.G. Cherkasova, M.R. Galding, L.V. Osetrova and Y.S. Varshavsky, *Rhodium Express* 1994, **3**, 17; (d) I.A. Poletaeva, T.G. Cherkasova, L.V. Osetrova, Y.S. Varshavsky, A. Roodt and J.G. Leipoldt, *Rhodium Express* 1994, **3**, 21.
- 26 C.A. Tolman, *Chem. Rev.* 1977, **77**, 313.
- 27 J.A. Venter, J.G. Leipoldt and R. van Eldik, *Inorg. Chem.* 1991, **30**, 2209.
- 28 (a) M. Sandström, I. Persson and P. Persson, *Acta Chem. Scand.* 1990, **44**, 653; (b) J. Rydberg, *Principles and practices of solvent extraction* (J. Rydberg, C. Musikas and G.R. Choppin, eds.), Marcel Dekker, New York, 1992, p. 23.